PLOS ONE

RESEARCH ARTICLE

Modeling vaccination strategies in an Excel spreadsheet: Increasing the rate of vaccination is more effective than increasing the vaccination coverage for containing COVID-19

Mario Moisés Alvarez[1,2]*, **Sergio Bravo-González**[1,2], **Grissel Trujillo-de Santiago**[1,3]

1 Centro de Biotecnología-FEMSA, Tecnologico de Monterrey, Monterrey, NL, México, **2** Departamento de Bioingeniería, Escuela de Ingeniería y Ciencias, Tecnologico de Monterrey, Monterrey, NL, México, **3** Departamento de Ingeniería Mecatrónica y Eléctrica, Escuela de Ingeniería y Ciencias, Tecnologico de Monterrey, Monterrey, NL, México

* mario.alvarez@tec.mx

Citation: Alvarez MM, Bravo-González S, Trujillo-de Santiago G (2021) Modeling vaccination strategies in an Excel spreadsheet: Increasing the rate of vaccination is more effective than increasing the vaccination coverage for containing COVID-19. PLoS ONE 16(7): e0254430. https://doi.org/10.1371/journal.pone.0254430

Editor: Muhammad Adrish, BronxCare Health System, Affiliated with Icahn School of Medicine at Mount Sinai, UNITED STATES

Received: January 13, 2021

Accepted: June 22, 2021

Published: July 19, 2021

Data Availability Statement: All relevant data are within the manuscript and its S1 Fig, S1 File and S1, S2 Tables.

Funding: MMA acknowledges the funding received from CONACyT (Consejo Nacional de Ciencia y Tecnología, México) through the Sistema Nacional de Investigadores (SNI scholarship 26048). GTdS acknowledges the funding received from CONACyT (Consejo Nacional de Ciencia y Tecnología,

Abstract

We have investigated the importance of the rate of vaccination to contain COVID-19 in urban areas. We used an extremely simple epidemiological model that is amenable to implementation in an Excel spreadsheet and includes the demographics of social distancing, efficacy of massive testing and quarantine, and coverage and rate of vaccination as the main parameters to model the progression of COVID-19 pandemics in densely populated urban areas. Our model predicts that effective containment of pandemic progression in densely populated cities would be more effectively achieved by vaccination campaigns that consider the fast distribution and application of vaccines (i.e., 50% coverage in 6 months) while social distancing measures are still in place. Our results suggest that the rate of vaccination is more important than the overall vaccination coverage for containing COVID-19. In addition, our modeling indicates that widespread testing and quarantining of infected subjects would greatly benefit the success of vaccination campaigns. We envision this simple model as a friendly, readily accessible, and cost-effective tool for assisting health officials and local governments in the rational design/planning of vaccination strategies.

Introduction

COVID-19 vaccines are finally in reach. In December 2020, the vaccines from Pfizer-BioNTech and Moderna-NIH were approved [1–3], after an unprecedentedly intense and rapid vaccine research campaign. Both of these vaccines are based on mRNA technology [2, 4–6] and exhibit efficacies of nearly 95%, as evaluated in clinical trials [7]. As vaccination campaigns have started already around the globe (e.g., in England, USA, Canada, and México), these and other vaccines are expected to obtain approval during 2021 in different countries.

The availability of approved vaccines provides certainty in the international quest to contain the greatest pandemic that we have experienced in modern times. However, the

México) through the Sistema Nacional de Investigadores (SNI scholarship 256730). SBG acknowledges the funding received from CONACyT (Consejo Nacional de Ciencia y Tecnología, México) in the form of a scholarship for doctoral studies. All authors acknowledge the funding provided by Tecnológico de Monterrey. The funders did not play any role in the study design, data collection and analysis, decision to publish, or preparation of the manuscript.

Competing interests: The authors have declared that no competing interests exist.

widespread deployment of vaccines still faces some challenges [8]. The extent and rate of vaccination in each country, and even in each city, will be determined by the global rate of vaccine manufacturing, the local logistics of distribution and application, and even public perception [9]. The cost of vaccines and vaccination campaigns is another aspect that will define the final availability (rate and coverage) of vaccines in a particular community. In the end, each country will have to design its own vaccination strategy based on cost, availability, public perceptions, and logistic considerations. A few economies will be able to implement fast and wide-coverage vaccination campaigns aimed at controlling COVID-19 progression within a few months. For most countries, vaccine campaigns will have to be sustained long-term efforts that extend throughout at least most of 2021 due to logistic limitations or cost (Moderna´s vaccine will cost ~25 pounds per dose; Pfizer´s vaccine will cost ~15 pounds per dose) [7].

In this context, relevant questions related to the impact of different vaccination strategies remain unanswered. What fraction of the population do we have to cover in a vaccination campaign? How much does the rate of vaccination matter? After vaccination starts, how soon can we go back to our "normal" lives? Are social distancing and widespread testing still needed through the vaccination period?

Intuitively, we can infer the qualitative answer to some of these questions. After all, a vaccine is not effective immediately after application, and herd immunity will be only evident after a significant fraction of the population is immune [10]. Both of the firstly approved vaccines (Pfizer-BioNTech and Moderna-NIH) have a high efficacy of η~0.95 [7, 11]. While individuals develop protective antibodies even after the first dose (i.e., η~0.50 efficacy, as demonstrated through clinical trials [5]), they require administration of two doses in a time frame of 21 or 30 days to reach a protection of 95% [5]. During that post-vaccination but pre-immune period, the pandemic will evolve, as a dynamic process driven by infective subjects (symptomatic and asymptomatic) that have not been diagnosed and quarantined and continue spreading the virus among the susceptible (not yet immune) population. Therefore, the interplay between vaccination and COVID-19 evolution in a particular community is a dynamic process, where several different rates compete.

The relevant rates are the local rate of infection, as influenced by the effectiveness of social distancing measures, the rate of testing and effective quarantining of infected subjects, and the rate of acquired immunity due to SARS-CoV-2 infection or vaccination. In turn, the rate of infection is affected by the effectiveness of all social distancing measures in that community. In principle, all these rates have to be considered when attempting to render an accurate forecast of the evolution of COVID-19 in a particular territory. Several studies [12, 13] have used mathematical modeling to investigate the role of vaccine efficacy and vaccine coverage in the attenuation of the pandemic progression. However, one aspect that remains poorly explored is the assessment of the effect of different vaccination rates on the progression of COVID-19. Again, the effect of the rate of vaccination must be analyzed in the context of the dynamic process of infection and in consideration of the effect of the social distancing and testing efforts as well.

Recently, we introduced an epidemiological model formulation that explicitly considers demographic variables and epidemiological parameters to calculate the progression of COVID-19 in urban areas [14]. This model can certainly be described as a variation of the original compartmental model first introduced by McKendrick and Kermack [15] or a variation of the SIR models very commonly used in the context of epidemiology [10, 16]. Compartmental models describe the interplay between different subsets of individuals in an epidemiological situation (infected symptomatic, asymptomatic, recovered, retrieved, deceased). However, the present model exhibits important differences in the definition of these compartments with respect to other models (i.e., we include the concept of retrieved subjects), the formulation of its parameters (i.e., we define a rate of infection instead of a

reproduction number (R)), and it allows for the easy incorporation of features (i.e., the testing effort and the vaccination rate). The model also considers the effectiveness of social distancing measures and of massive testing for expeditious identification and quarantining of infective subjects as inputs, which is not straightforward in conventional SIR models [16].

In this communication, we have modified our original formulation to include the effect of vaccination coverage and rate, and we use this simple model to predict the pandemic progress in highly populated cities. We present a wide range of simulation scenarios for a hypothetical urban area, and we evaluate the relative effect of different schemes of vaccination (i.e., combinations of social distancing, testing intensity, and vaccination coverage and rate) on the evolution of COVID-19.

Materials and methods

Mathematical model

We used a simple epidemiological model for the propagation of COVID-19 in urban areas that considers two variable populations of individuals, infected (X(t)) and retrieved (R(t)) (Fig 1; S1 File).

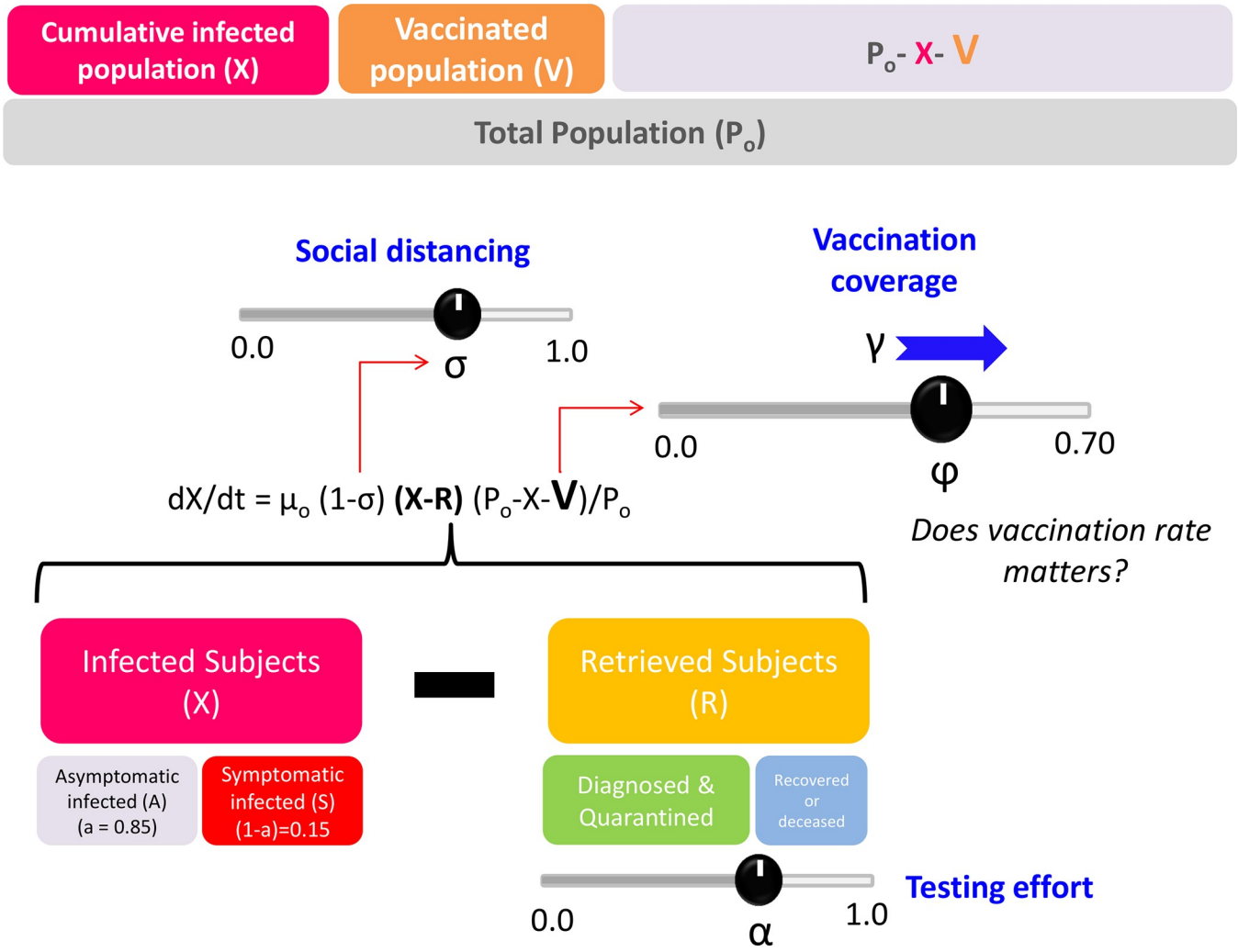

Fig 1. Do vaccination rates matter? Schematic representation of a demographic mathematical model that considers social distancing (σ), intensity of the testing effort (α), vaccination coverage (φ), and vaccination rate (γ) to predict the evolution of pandemic COVID-19 in urban areas.

https://doi.org/10.1371/journal.pone.0254430.g001

The model is based on a set of two simple differential equations.

$$dX(t)/dt = \mu_o(1-\sigma(t))\ (X(t)-R(t))\ (P_o-X(t)-V(t))/P_o \quad \text{Eq (1)}$$

$$dR(t)/dt = \alpha(X(t))|_{t-delay_q} + (1-\alpha)(X)|_{t-delay_r} \quad \text{Eq (2)}$$

The first equation describes the rate of new infections (X(t)). This rate of accumulation of infected habitants (asymptomatic and symptomatic) in an urban area (assumed to be a closed system) is proportional to the number of infective subjects present in that population at a given point (X(t)-R(t)) and the fraction of the population still susceptible to infection ((P_o-X(t)-V(t))/P_o). The second accounts for the rate of accumulation of retrieved (R(t)) subjects from the infective population. The number of retrieved subjects is defined as the number of inhabitants that have been retrieved from the general population and therefore are not contributing to the propagation of COVID-19. Subjects are "retrieved" from the infective population either because they have been effectively isolated from the non-infected population (i.e., hospitalized or quarantined after positive diagnosis), they have recovered from COVID-19 and are no longer infectious, or they have died.

Note that in this model, the quantity (X(t)-R(t)) is the driving force that sustains the local evolution of the pandemics. The number of infective subjects is given by the difference between the accumulated number of infected subjects (X(t)) and the number of retrieved subjects (R(t)).

The proportionality constant in Eq 1 (μ_o) is an intrinsic rate of infection. However, this rate of generation of new cases is modulated by several factors, including the effective degree of activity in the region (1-σ(t)). Here, σ is a fraction that denotes the effective decrease in human activity or mobility in the region (or the effective decrease in demographic density) caused by the set of social distancing countermeasures (σ(t)) currently established among that population (i.e., restrictions in social and economic activities, use of masks, restrictions in mobility, and all measures that contribute to an effective decrease in demographic density).

The fraction of the susceptible population decreases over time, as more inhabitants in the community get infected (X(t)) or are vaccinated (V(t)). Then, the model also considers that the rate of generation of new cases is modulated by the fraction of the population that is susceptible to the infection (P_o-X(t)-V(t))/P_o. This is precisely where the number of vaccinated subjects (V(t)) plays a role by reducing the pool of susceptible individuals.

The second equation (Eq 2) describes the rate at which infected patients are retrieved from the infective population. Eventually, all infected subjects are retrieved from the population of infected individuals, but this occurs at distinct rates. A fraction of infected individuals (α) is effectively retrieved from the general population soon after the onset of symptoms or after a positive diagnosis. Another fraction of infected subjects (1- α) is not effectively retrieved from the population until they have recovered or died from the disease. Therefore, in our formulation, the overall rate of retrieval (dR/dt) has two distinctive contributions, each one associated with different terms on the right-hand side of Eq 2. The first term accounts for the active rate of retrieving infected patients through the diagnosis and quarantine of SARS-CoV-2 positive subjects. For this term, the delay from the onset of virus shedding to positive diagnosis and quarantine (delay_q) is considered short (*i.e.*, between two to five days), to account for a reasonable time between the positive diagnosis and the action of quarantine. In our model formulation, this term is represented by (1-α). A second term relates to the recovery or death of infected patients (symptomatic or asymptomatic) and is represented by the integral of all infected subjects recovered or deceased from the onset of the epidemic episode in the region,

considering a delay of 14 days (delay_r), which accounts for the average time of recovery of an infected individual.

Note that the simultaneous solution of Eqs 1 and 2 is sufficient to describe the evolution of the number of asymptomatic individuals (A), symptomatic individuals (S), and deceased patients (D) through the specification of several constants and simple relations.

$$a\ dX/dt = dA/dt \quad \text{Eq (3)}$$

$$(1-a)\ dX/dt = dS/dt \quad \text{Eq (4)}$$

$$m\ [(1-a)\ dX/dt] = dD/dt \quad \text{Eq (5)}$$

Here, **a** is the fraction of asymptomatic subjects among the infected population, (1-**a**) is the fraction of infected individuals that exhibit symptoms, and **m** the mortality rate expressed as a fraction of symptomatic individuals. Note tt a delay should be used to properly model the number of deaths with time. In its current form, our model predicts the number of deaths associated with people getting infected in the current time.

Parameter values and assumptions

This model relies on some basic assumptions that are sustained in clinical or epidemiological data.

The clinical parameters include an intrinsic infection rate constant (μ_o) that can be calculated from the initial stage of the pandemic in that particular region, the fraction of asymptomatic patients (α), the delay between the period of viral shedding by an infected patient (delay_r), the period from the onset of shedding to the result of first diagnosis and quarantine in the fraction of patients effectively diagnosed (delay_q), and the fraction of infected patients effectively diagnosed and retrieved from the population ($\alpha(t)$). Demographic parameters include the population of the region (P_o), the effect of social distancing ($\sigma(t)$) in terms of effectively decreasing the demographic density, the fraction of infected individuals retrieved from the population due to massive and effective testing ($\alpha(t)$), and the vaccine coverage (φ) and vaccination rate (γ).

For illustrative purposes, we set the value of μ_o (the intrinsic rate of infection) in 0.33 day^{-1} in our simulations. This value is similar to that observed in Sao Paulo (~0.308), Mexico City (~0.329), Toronto (~0.330), Lisbon (~0.341), Madrid (~0.358) and London (0.362), at the local onset of pandemic COVID-19 in 2020. Other urban areas have exhibited values of μ_o between 0.2 and 0.65 day^{-1} (S1 Table). The value of μ_o (i.e., the intrinsic rate of infectivity of SARS-CoV2 before interventions) can be calculated for any urban area assuming that the initial rate of propagation is $d(X)/dt = \mu_o [X]$, where [X] is the number of initially infected subjects [14]. Subsequently, the intrinsic rate of infection can be calculated from the initial slope of a plot of ln [X] *vs* time, which is a usual procedure for the calculation of intrinsic growth rates in cell culture scenarios under the assumption of a first-order rate growth dependence.

The fraction of asymptomatic infected (a) is one of the critical inputs for the model; it determines the final and maximum feasible threshold of symptomatic infected. The current evidence is not yet sufficient to support a conclusive value for this parameter. For the simulations presented here, we set a = 0.85, based on a recent serological study conducted in New York City (NYC) that found anti-SARS-CoV-2 IGGs among 21.2% of the population [17]. This serological result, combined with simulation work, suggests that nearly 85% of exposed New Yorkers were asymptomatic or exhibited minor symptoms. In addition, the average time of infectiousness was set at 14 days in our simulations. Viral shedding can last for three to four

weeks after the onset of symptoms [18]. However, according to current recommendations and clinical guidelines, most ambulatory patients are generally considered COVID recovered and no longer infectious after day 10 (from the onset of symptoms) unless they are immune compromised. This recommendation is consistent with recent reports that correlate SARS-CoV-2 infectivity in cell cultures versus CT values in PCR results of infected subjects during the first 10 days of infection [19]. Based on more conservative sources [20, 21], we adopted a period of infectiveness of 14 days after infection for the simulations presented here. Similarly, asymptomatic patients are only removed from the pool of susceptible persons 14 days post infection. Asymptomatic patients are considered part of the population capable of transmitting COVID-19; reported evidence that suggests that asymptomatic subjects (or minimally symptomatic patients) may exhibit similar viral loads [22] to those of symptomatic patients and may be active transmitters of the disease [23, 24].

The model also requires the definition of the mortality rate (m) associated with COVID-19.

The worldwide average fraction of patients that die as a consequence of COVID-19 is estimated to be 0.029 of those infected 21 days before [25]. We also consider that the average time for bed occupancy of hospitalized patients is 14 days. The estimated average hospitalization stays range from 9.3 to 13 days in the United States [26] and China [27, 28], but much longer stays were reported in intensive care units in Italy (20 to 25 days) [29]. Anecdotal data collected in México suggests that hospitalization stays of at least two weeks are a more accurate figure for Latin American societies.

The model assumes that infection results in short-term immunity upon recovery (at least 12 months). This assumption is based in experimental evidence that suggests that rhesus macaques that recovered from SARS-CoV-2 infection could not be reinfected [30]. However, the acquisition of full immunity to reinfection has not been confirmed in humans, although it is well documented for other coronavirus infections, such as SARS and Middle East respiratory syndrome (MERS) [31, 32].

Results and discussion

Using this simple epidemiological model, our aim was to reproduce representative settings for COVID-19 progression. For illustrative purposes, we have selected a representative urban area (i.e., more than 1,000,000 inhabitants and a population density above 4,000 habitants km^{-2}). In all our simulations, we calculated the number of symptomatic subjects, the number of new cases per 1,000,000 of inhabitants, and the maximum hospital bed occupancy in that hypothetical region.

For all simulations presented here, we assumed that vaccination occurs immediately after the pandemic onset. We also assume that social distancing is in effect during the entire vaccination campaign so that the level of activity in the city is decreased (and therefore the effective population density) by 50% (i.e., $\sigma = 0.50$). Our simulations suggest that even aggressive vaccination campaigns (i.e., 70% vaccine coverage in 1.5 months) do not have substantial effects in the absence of social distancing and that they have only minor effects (S1 Fig) even at moderate degrees of social distancing (i.e., $\sigma = 0.25$).

We explored the range of vaccination coverage from 30% to 70%. Recent reports suggest that a vaccination coverage higher than 70% may be unattainable simply due to public perceptions [33]. In surveys conducted in 28 nations, a pooled average of 20% of the participants expressed their intention to refuse SARS-CoV-2 vaccination. In addition, vaccine manufacturing is expected to be at a developing stage during 2021 [8]. Therefore, in all probability, the rate of manufacture of vaccines will be lower than their demand at least during the current year. In this context, reaching vaccine coverage higher than 70% seems challenging for most countries.

In a first set of simulations (Fig 2A and 2B), we investigated the effect of different rates of vaccination at fixed vaccination coverage under the following set of common assumptions: (a) the overall vaccination coverage will be limited to 30% of the population; (b) the intrinsic rate of infection is $\mu_o = 0.33$, similar to actual values observed in densely populated urban areas, such as Mexico City and Madrid (S1 Table); and (c) σ, the effective value of social distancing, is equal to 0.5. Vaccination consists of the application of two vaccine dosages during 30 days. In this contribution, we assumed that vaccinated subjects will acquire 50% protection 14 days after receiving the first dose and will exhibit a 90% protective level of anti-SARS-CoV-2 antibodies only at ~30 to 45 days after they received the first dose.

In addition, for these sets of simulations, the testing effort is such that only 15% of the infected subjects are tested and quarantined, while the rest of the infected subjects continue to be active until recovery. This strategy is consistent with that adopted by countries that have diagnosed essentially only those subjects who were symptomatic and asked for medical assistance (i.e., México, Chile, and Bolivia, with fewer than 2 tests per confirmed case) [34].

Under this set of assumptions, we explored three different rates of vaccination (Fig 2A and 2B) to cover 30% of the population ($\varphi = 0.3$) in 1 year (orange curves; $\gamma = P_o\ year^{-1}$), in 6 months (grey curves; $\gamma = 2\ P_o\ year^{-1}$), and in 3 months (yellow curves; $\gamma = 4\ P_o\ year^{-1}$). These three rates of vaccination are equivalent to coverage of 100% P_o in one year ($\gamma = P_o\ year^{-}$), six months ($\gamma = 2\ P_o\ year^{-}$), or three months ($\gamma = 4\ P_o\ year^{-}$).

The pandemic progression (number of cumulative symptomatic cases, and new infections per day) is indicated with blue curves for a reference scenario with a social distancing of 50% (i.e., an effective decrease of 50% in the demographic density) and a basal level of testing (i.e., only 15% of the infective subjects are tested and quarantined, while the rest of the infected subjects continue active until recovery). The results of our simulations show that increasing the rate of vaccination has a prominent effect on the epidemic curve. Fig 2A shows the cumulative number of symptomatic cases at different vaccination rates when the vaccine coverage is limited to 30%. Fig 2B shows the new number of symptomatic cases per day at different vaccination rates and 30% coverage. The vaccination rate has a clear effect on both the shape and the area of the epidemic curves. Note that the peak of new infections is substantially lower as the vaccination rate is increased.

The total number of expected symptomatic cases (Fig 2A), the peak of new infections (Fig 2B), and the maximum bed occupation at hospitals (inset in Fig 2B) progressively and substantially decreased as the vaccination rate is increased. Evidently, a great benefit is attained by accelerating the distribution and application of vaccine as much as possible. The scenario of achieving a 30% coverage (300,000 vaccines per million of habitants) in three or six months seams feasible and reduces the overall number of symptomatic infected and the bed maximum bed occupancy in nearly 70% and 40%, respectively, with respect to the base case.

Fig 2C and 2D show the cumulative number of cases and the number of new infections per day, respectively, at different vaccination rates and at a vaccine coverage of 50% ($\varphi = 0.5$). The maximum bed occupancy under this scenario is shown in the inset of Fig 2D. As before, we included a base case (blue curves) in which no vaccination occurs, whereas social distancing still has an effect equivalent to a decrease of 50% in the demographic density, and 15% of the infective subjects are diagnosed and quarantined.

Similarly, Fig 2E and 2F show the cumulative number of cases and the number of new infections per day, respectively, at different vaccination rates and at a vaccine coverage of 70% ($\varphi = 0.7$). The pandemic indicators (i.e., overall number of symptomatic subjects, peak of new cases per day and maximum bed occupancy) decrease modestly as vaccine coverage is increased from $\varphi = 0.30$ to 0.50 or even 0.70. The benefit of increasing vaccine coverage at a given vaccination rate is substantially smaller than the benefit of increasing the rate of

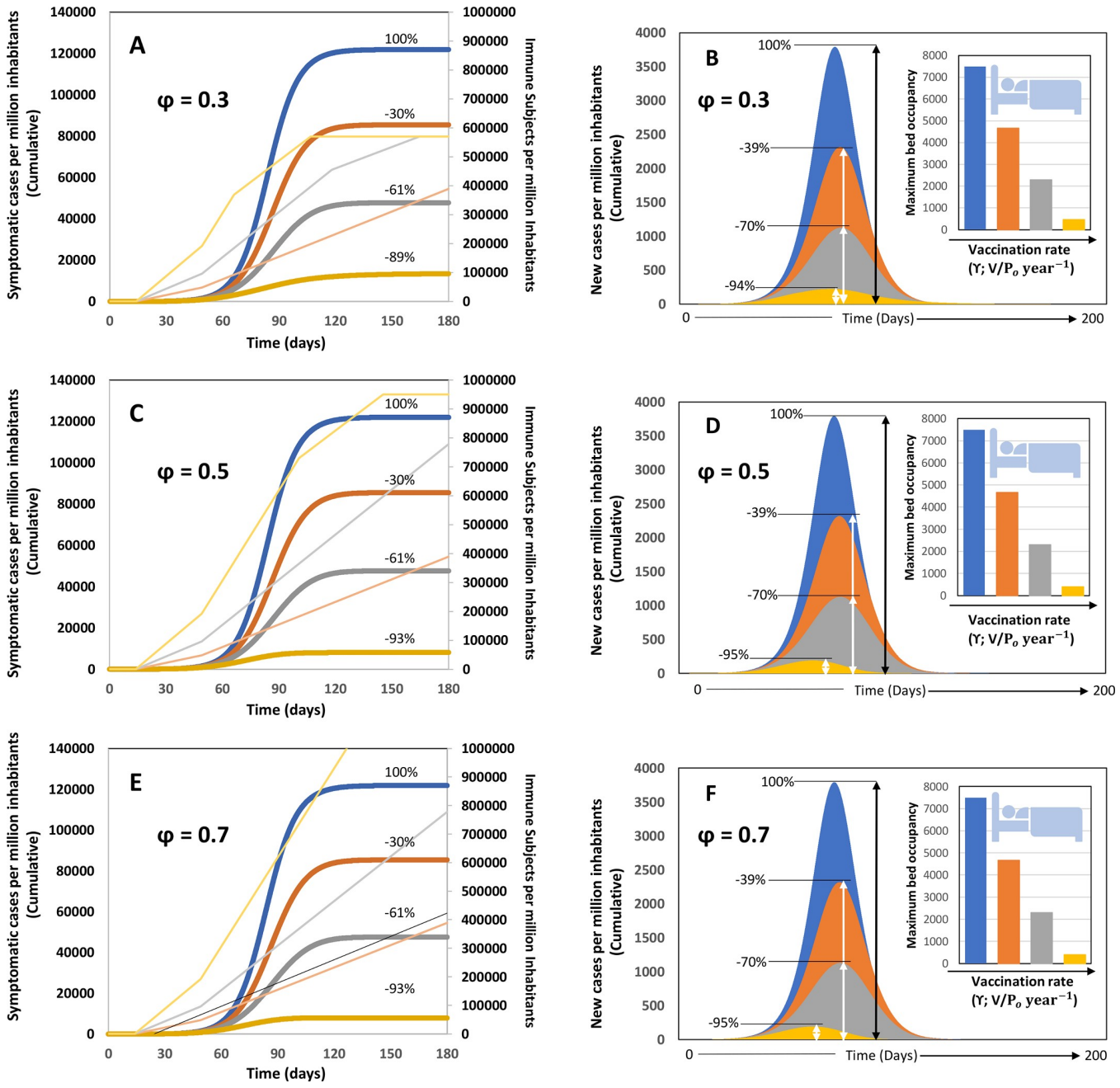

Fig 2. Scenarios of pandemic evolution for vaccination at different values of vaccination coverage and vaccination rates and under conditions of moderate social distancing (i.e., 50%) and basal values of testing effort (i.e.; α = 0.15). (A) Cumulative number of infections, (B) daily number of new symptomatic cases and maximum bed occupancy (inset) for vaccination scenarios in which the vaccine coverage is kept constant at 30% P_o (φ = 0.30), the effectiveness of the social distancing measures is 50% (σ = 0.50), a basal level of testing is established (α = 0.15). (C) Cumulative number of infections, (D) daily number of new symptomatic cases and maximum bed occupancy (inset) for vaccination scenarios in which the vaccine coverage is kept constant at 50% P_o (φ = 0.50; σ = 0.50; and α = 0.15). (E) Cumulative number of infections, (F) daily number of new symptomatic cases and maximum bed occupancy (inset) for vaccination scenarios in which the vaccine coverage is kept constant at 70% P_o (φ = 0.70; σ = 0.50; and α = 0.15). For all these cases, different vaccination rates such that: the entire population could be vaccinated within a year (vaccination at $\gamma = P_o$ year^{-1}; orange curve); within six months (vaccination at $\gamma = 2\ P_o$ year^{-1}; grey curve); or within three months (vaccination at $\gamma = 4\ P_o$ year^{-1}; yellow curve). A reference scenario without vaccination is included in all panels (blue curve). Numbers indicate the percentage of reduction of symptomatic cases that results from the application of each vaccination rate with respect to the reference case. The number of immune subjects at different times, in accordance with different vaccination rates, is indicated with the same color code in the secondary axis.

https://doi.org/10.1371/journal.pone.0254430.g002

vaccination at a fixed vaccination coverage. Indeed, our results suggest that the overall vaccine coverage of 30% of the population at a rate of 100% P_o in 6 months is more effective than the vaccine coverage of 50% of the population at a rate of 100% P_o in one year, in terms of controlling the number of infections. Note that even increasing the coverage to 70% at the lowest rate does not provide the same benefits as a coverage of 50% achieved over a shorter period (e.g., 6 or 3 months). A modest coverage of 30% of the population at a rate of 100% P_o in 6 months provides better results than a higher coverage of 70% at a rate of 100% P_o in an entire year. Results suggest that a high vaccination coverage implemented at a slow rate is not able to exceed the rate of new infections. A modest coverage (i.e., 30%) executed in a very short time (such as the strategy followed by the USA or Israel) delivers more vaccines per day than a slow and high coverage vaccination. Therefore, modest but fast is more effective than ambitious and slow, in this case.

Fig 3 presents predictions for scenarios where 50% social distancing is implemented, but where the level of diagnostic testing is increased from a basal value (15% of infected are diagnosed and quarantined) to situations were 30% of infected patients (symptomatic and asymptomatic) are diagnosed within the first 5 days of viral shedding and are quarantined. This set of results allows observation of the effect of testing intensification combined with social distancing and vaccination. This would be a more realistic and recommended scenario. As before, the trends related to the reference scenario of 30% testing ($\alpha = 0.30$) and 50% social distance enforcement ($\sigma = 0.50$) are indicated in blue. The combination of moderate testing and vaccination renders better results than is achieved with basal testing and vaccination. The estimate of maximum bed occupancy is reduced by at least 50% for all values of vaccination coverage and vaccination rates analyzed. For example, at the feasible scenario of 50% coverage at 100% P_o in 6 months, the maximum bed occupancy decreases from 5800 to 900 beds if a moderate testing effort ($\alpha = 0.30$) is in place.

As before, increasing the rate of vaccination is more efficacious than simply increasing vaccination coverage at a slow vaccination rate. For example, a vaccination strategy aimed at reaching 50% of the population at a rate of 100% P_o in 6 months results in the maximum bed occupancy of ~900 beds. By contrast, increasing the coverage to 70% at a rate of 100%P_o in one year yields a higher maximum bed occupancy (~2824 beds).

A graphical summary of the results for different combinations of scenarios is presented in Fig 4. The effect of different vaccination rates is shown in terms of the number of symptomatic individuals at different vaccine coverage in (Fig 4A) and the maximum bed occupancy (Fig 4B). Lines drawn in different colors indicate the different values of vaccine coverage (i.e., 30%, 50%, and 70%). The vaccination rate exhibits a dominant effect on the parameters of the local evolution of the COVID-19 pandemic and defines the number of symptomatic cases (Fig 4A) and the maximum bed occupancy (Fig 4B). Covering 70, 50, or 30% of the population at vaccination rates of 100% P_o in 12 or 6 months renders practically equivalent results. A higher vaccination coverage (50–70%) renders higher benefits than the lowest vaccination coverage (30%) only at the highest vaccination rate evaluated (i.e., vaccinating 100% P_o in 3 months).

In Fig 4A and 4B we selected a reduced set of scenarios to illustrate relevant relationships between vaccination rate and coverage and reduction in some of the indicators of the local evolution of pandemic COVID-19. However, the demographic model that we used is flexible enough to simulate a wide range of additional scenarios that combine social distancing, testing effort, vaccination coverage and rate, and vaccination efficacy (S2 Table).

For example, Fig 4C and 4D present an analysis of the effect of the use of vaccines with different efficacies (i.e., $\eta = 0.95$, 0.90, and 0.70). This type of analysis may be highly useful for this and other epidemic emergencies since constraints in the availability, cost, or logistics of

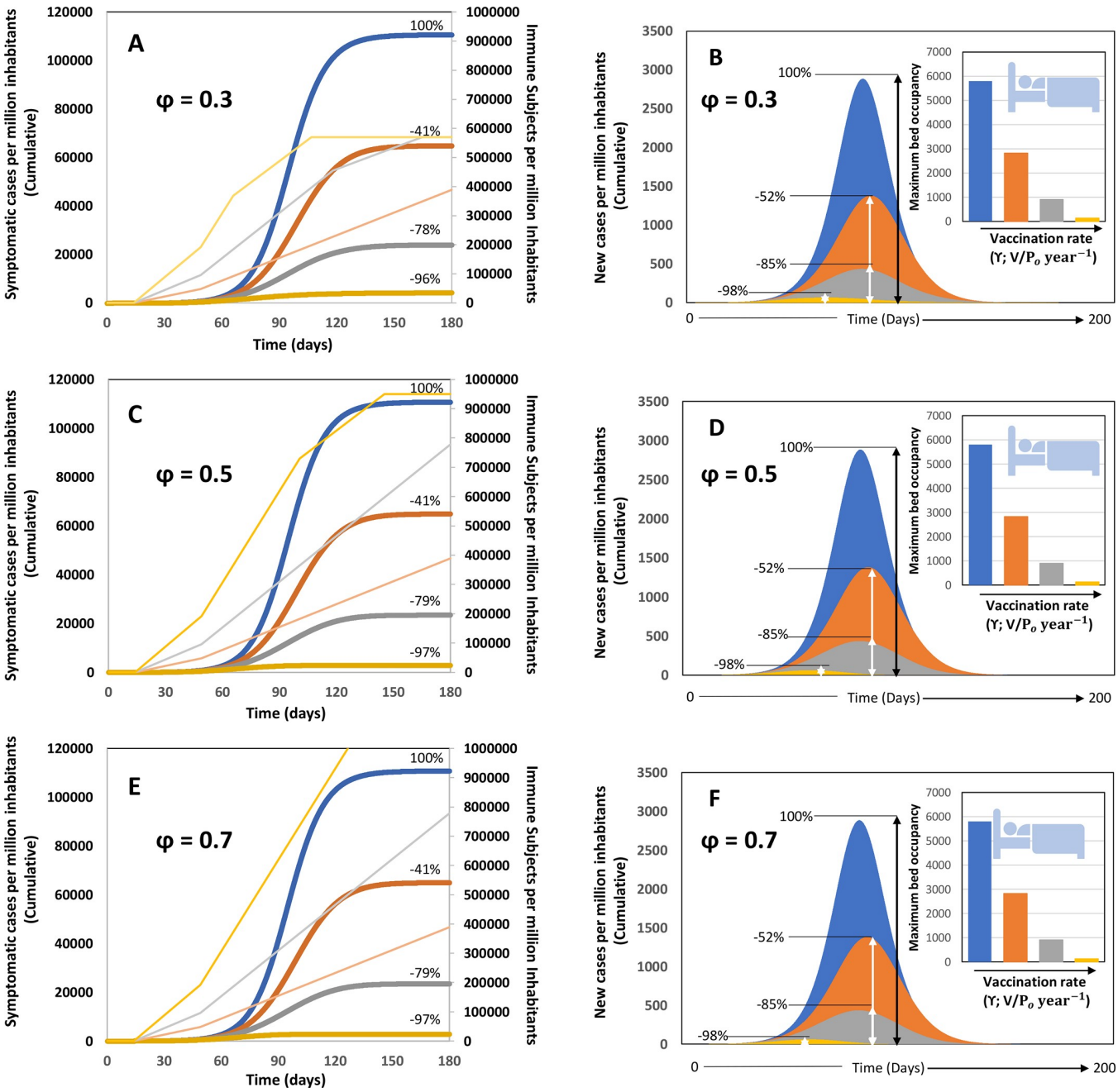

Fig 3. Scenarios of pandemic evolution for vaccination at different values of vaccination coverage and vaccination rates and under conditions of moderate social distancing (i.e., 50%) and enhanced testing effort (i.e., α = 0.30). (A) Cumulative number of infections, (B) daily number of new symptomatic cases and maximum bed occupancy (inset) for vaccination scenarios in which the vaccine coverage is kept constant at 30% P_o (φ = 0.30), the effectiveness of the social distancing measures is 50% (σ = 0.50), a moderate level of testing is established (α = 0.30). (C) Cumulative number of infections, (D) daily number of new symptomatic cases and maximum bed occupancy (inset) for vaccination scenarios in which the vaccine coverage is kept constant at 50% P_o (φ = 0.50; σ = 0.50; and α = 0.30). (E) Cumulative number of infections, (F) daily number of new symptomatic cases and maximum bed occupancy (inset) for vaccination scenarios in which the vaccine coverage is kept constant at 70% P_o (φ = 0.70; σ = 0.50; and α = 0.30). For all these cases, different vaccination rates such that: the entire population could be vaccinated within a year (vaccination at $\gamma = P_o$ year^{-1}; orange curve); within six months (vaccination at $\gamma = 2\ P_o$ year^{-1}; grey curve); or within three months (vaccination at $\gamma = 4\ P_o$ year^{-1}; yellow curve). A reference scenario without vaccination is included in all panels (blue curve). Numbers indicate the percentage of reduction of symptomatic cases that results from the application of each vaccination rate with respect to the reference case. The number of immune subjects at different times, in accordance with different vaccination rates, is indicated with the same color code in the secondary axis.

https://doi.org/10.1371/journal.pone.0254430.g003

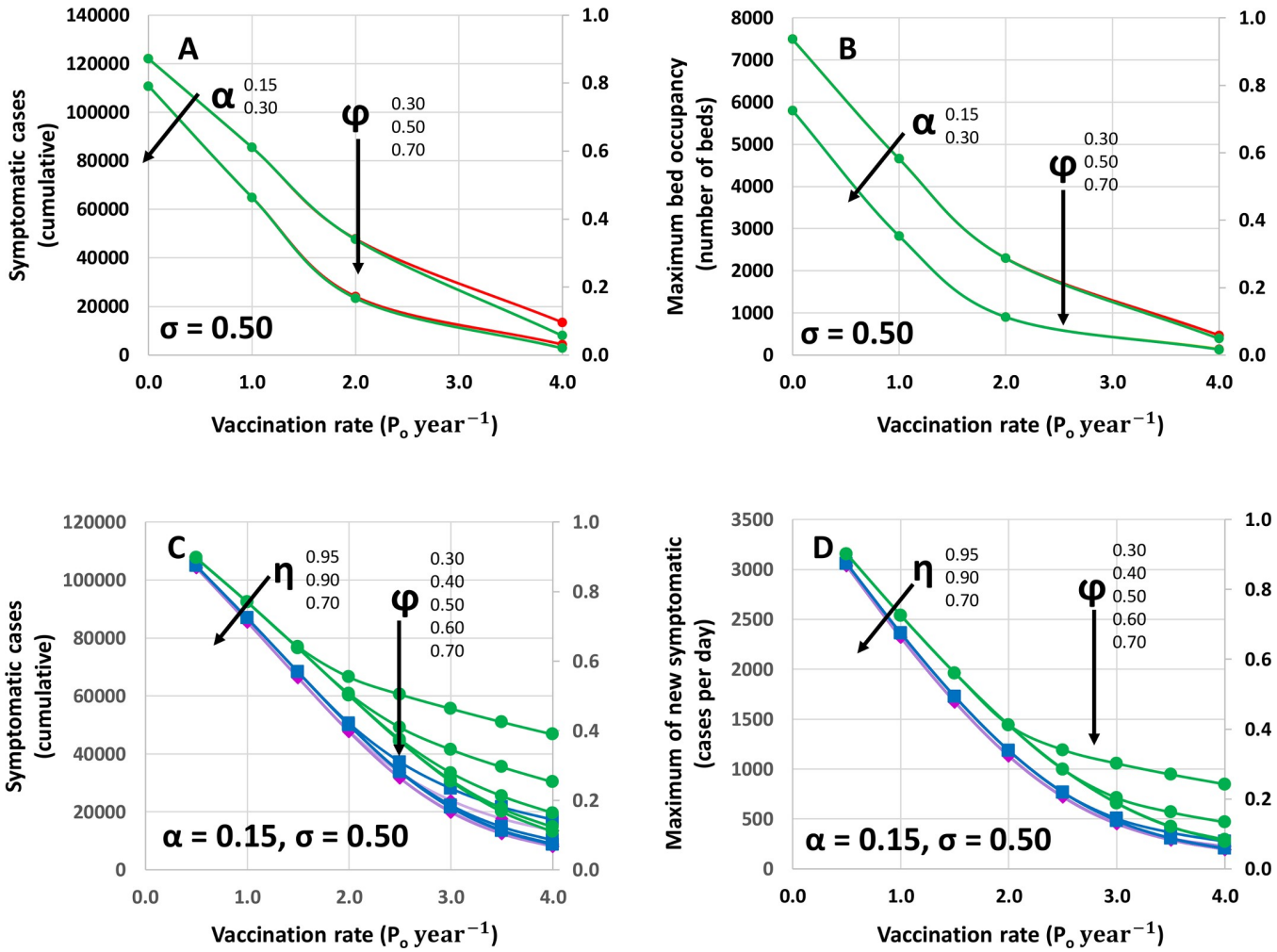

Fig 4. Effect of different values of vaccination coverage and vaccination rates on pandemic indicators. (A) Number of cumulative cases, and (B) maximum bed occupancy predicted in response to the application of different vaccination rates whereby the entire population could be vaccinated within a year (vaccination at $\gamma = P_o$ year^{-1}), within six months (vaccination at $\gamma = 2\ P_o$ year^{-1}), or within three months (vaccination at $\gamma = 4\ P_o$ year^{-1}) at different values of vaccine coverage: 30% P_o ($\phi = 0.30$: red), 50% P_o ($\phi = 0.50$: yellow), and 70% P_o ($\phi = 0.30$: green). Curves for two different values of the coefficient of testing effort are presented ($\alpha = 0.15$ and $\alpha = 0.30$). The secondary axis indicates fractional values with respect to the same reference (i.e., no vaccination, moderate social distancing ($\sigma = 0.50$), and basal testing effort ($\alpha = 0.15$). (C) Number of cumulative cases, and (D) maximum number of new symptomatic cases per day predicted in response to the application of different vaccination rates ($\gamma = 0.5\ P_o$ to 4.0 year^{-1}) and at different values of vaccine coverage (from 30% to 70%; $\phi = 0.30$ to 0.70). Curves for three different values of vaccination efficacies are presented ($\eta = 0.95$; magenta rhombs, $\eta = 0.90$; blue squares, and $\eta = 0.70$; green circles). The secondary axis indicates fractional values with respect to the same reference (i.e., no vaccination, moderate social distancing ($\sigma = 0.50$), and moderate testing effort ($\alpha = 0.30$).

https://doi.org/10.1371/journal.pone.0254430.g004

vaccine storage or distribution will require countries to fulfill their vaccination requirements using not one but several vaccine alternatives.

We illustrate the type of information that the model may provide in S2 Table. Five different indicators are calculated for different vaccination scenarios, including the day of the epidemic peak, the number of new infection cases at the epidemic peak, the cumulative number of symptomatic infections after 150 days of the local pandemic onset, the maximum bed occupancy, and the number of fatalities at different case fatality rates. Regardless of vaccination coverage, a fast vaccination rate (i.e., equal than or higher than 2 P_o) renders reductions of more than 60% of symptomatic cases and maximum bed occupancies.

Note that one of the limitations of our model is that we assume that all the individuals that receive the vaccine are still part of the susceptible pool (i.e., they have not yet been exposed to the virus). The error that we estimate from this assumption may be important in some cases. For example, in urban areas severely hit by COVID-19, less than 5% of the population has been infected. Therefore, for a modest vaccination coverage (i.e., 30%), the vaccination of people that have already been infected (symptomatic and asymptomatic) would decrease the effective vaccination coverage to $(0.30)\times(0.04/0.15) = 8.6\%$. This may imply that the intended vaccination coverage of 30%, 50%, and 75% probably result in an effective vaccination rate of ~ 21%, 35%, and 50% for the non-exposed population of largely affected regions. The model can be easily modified to correct this situation and to subtract previously immunized individuals from the vaccinated set.

Conclusions

Within the next weeks, each country will have to design its own vaccination strategy based on cost, availability, public perceptions, and logistic considerations. Here, we aim to provide a friendly, easy-to-use modeling tool to assist governments and local health officials to rationally design vaccination campaigns.

We constructed a simple demographic model based on two differential equations that follow the accumulation of the number of infected subjects and the number of subjects retrieved from the infective population. This model formulation is extremely flexible and enables the prediction of the evolution of pandemic COVID-19 in urban areas based on simple reported parameters related to COVID-19 epidemiology and under different scenarios that may consider different degrees of social distancing and/or intensities of the testing effort, and different vaccination strategies. In this study, we focus on analyzing the effect of different levels of vaccination coverage and different vaccination rates on the local progression of COVID-19 in an urban area.

Our results suggest that the rate of vaccination is highly relevant in controlling the evolution of COVID-19 in highly populated cities. Based on the predictions of our model, we recommend the implementation of vaccination campaigns capable of achieving an overall coverage of at least 50% in short time periods (ideally within 3 or 6 months). In general, a faster deployment of vaccines should be preferred over a higher vaccine coverage that implies slower vaccination rates. Our model predicts that a vaccination campaign covering only 50% of the population in 3 or 6 months is more effective in controlling COVID-19 progression than is a vaccination strategy with a final coverage of 70% in longer times.

Importantly, our results clearly show that social distancing measures, including the use of face masks and restriction of regular social and economic activities, must not be lifted during at least the first three months of any vaccination campaigns. Only the combination of social distancing and vaccination enables the control of COVID-19 progression in highly populated cities within a time frame of 3–4 months. In addition, the intensification of the testing effort during the implementation of vaccination campaigns yields relevant reductions in terms of decreasing maximum bed occupancy and the number of symptomatic cases.

Supporting information

S1 File. Implementation of the demographic mathematical model in an excel spreadsheet. (XLSX)

S1 Fig. Scenarios of pandemic evolution during the vaccination of 70% of the population at different vaccination rates under conditions of modest social distancing (i.e., 25%). (A)

The cumulative number of infections, (B) the number of new infections per day and the maximum bed occupancy (inset) are presented for vaccination scenarios in which the vaccine coverage is kept constant at 70% P_o ($\varphi = 0.70$), the effectiveness of the social distancing measures is 20% ($\sigma = 0.20$), a basal level of testing is established ($\alpha = 0.15$), and different vaccination rates are imposed, such that: the entire population could be vaccinated within a year (P_o $year^{-1}$; orange curve), within six months (2 P_o $year^{-1}$; grey curve), or within three months (vaccination at 4 P_o $year^{-1}$; yellow curve). A reference scenario without vaccination is included (blue line). Numbers indicate the percentage of reduction of symptomatic cases that results from the application of each vaccination rate with respect to the reference case.
(TIFF)

S1 Table. Specific infection rates (μ_o) and the associated doubling times (t_d) for COVID-19 infection in different geographic regions. The intrinsic rate of infection ranges between 0.30 and 0.37 for territories with population densities between 4,000 and 7,000 hab km^2.
(DOCX)

S2 Table. Effect of different vaccination scenarios in relevant indicators of the local evolution of pandemic COVID-19. Indicators are calculated for different vaccination scenarios, including the day of the epidemic peak, the number of new infection cases at the epidemic peak, the cumulative number of symptomatic infections after 150 days of the local pandemic onset, the maximum bed occupancy, and the number of fatalities at different case fatality rates.
(DOCX)

Author Contributions

Conceptualization: Mario Moisés Alvarez, Grissel Trujillo-de Santiago.

Data curation: Mario Moisés Alvarez.

Formal analysis: Mario Moisés Alvarez, Grissel Trujillo-de Santiago.

Funding acquisition: Mario Moisés Alvarez, Grissel Trujillo-de Santiago.

Investigation: Mario Moisés Alvarez, Sergio Bravo-González, Grissel Trujillo-de Santiago.

Methodology: Mario Moisés Alvarez, Sergio Bravo-González, Grissel Trujillo-de Santiago.

Project administration: Mario Moisés Alvarez, Grissel Trujillo-de Santiago.

Resources: Mario Moisés Alvarez.

Software: Mario Moisés Alvarez.

Supervision: Mario Moisés Alvarez, Grissel Trujillo-de Santiago.

Writing – original draft: Mario Moisés Alvarez.

Writing – review & editing: Mario Moisés Alvarez, Grissel Trujillo-de Santiago.

References

1. Oliver SE, Gargano JW, Marin M, Wallace M, Curran KG, Chamberland M, et al. The Advisory Committee on Immunization Practices' Interim Recommendation for Use of Moderna COVID-19 Vaccine—United States, December 2020. MMWR Morb Mortal Wkly Rep. 2021; 69: 1653–1656. https://doi.org/10.15585/mmwr.mm695152e1 PMID: 33382675
2. Tanne JH. Covid-19: FDA approves Moderna vaccine as US starts vaccinating health workers [Internet]. The BMJ. BMJ Publishing Group; 2020. https://doi.org/10.1136/bmj.m4924
3. Tanne JH. Covid-19: FDA panel votes to approve Pfizer BioNTech vaccine. BMJ. NLM (Medline); 2020; 371: m4799. https://doi.org/10.1136/bmj.m4799 PMID: 33310748

4. Jackson LA, Anderson EJ, Rouphael NG, Roberts PC, Makhene M, Coler RN, et al. An mRNA Vaccine against SARS-CoV-2—Preliminary Report. N Engl J Med. Massachusetts Medical Society; 2020; 383: 1920–1931. https://doi.org/10.1056/NEJMoa2022483 PMID: 32663912

5. Polack FP, Thomas SJ, Kitchin N, Absalon J, Gurtman A, Lockhart S, et al. Safety and Efficacy of the BNT162b2 mRNA Covid-19 Vaccine. N Engl J Med. Massachusetts Medical Society; 2020; 383: 2603–2615. https://doi.org/10.1056/NEJMoa2034577 PMID: 33301246

6. Baden LR, El Sahly HM, Essink B, Kotloff K, Frey S, Novak R, et al. Efficacy and Safety of the mRNA-1273 SARS-CoV-2 Vaccine. N Engl J Med. Massachusetts Medical Society; 2020; NEJMoa2035389. https://doi.org/10.1056/NEJMoa2035389 PMID: 33378609

7. Mahase E. Covid-19: What do we know about the late stage vaccine candidates? BMJ. NLM (Medline); 2020; 371: m4576. https://doi.org/10.1136/bmj.m4576 PMID: 33234507

8. Anderson RM, Vegvari C, Truscott J, Collyer BS. Challenges in creating herd immunity to SARS-CoV-2 infection by mass vaccination [Internet]. The Lancet. Lancet Publishing Group; 2020. pp. 1614–1616. https://doi.org/10.1016/S0140-6736(20)32318-7 PMID: 33159850

9. Mello MM, Silverman RD, Omer SB. Ensuring Uptake of Vaccines against SARS-CoV-2. N Engl J Med. Massachusetts Medical Society; 2020; 383: 1296–1299. https://doi.org/10.1056/NEJMp2020926 PMID: 32589371

10. Randolph HE, Barreiro LB. Herd Immunity: Understanding COVID-19. Immunity. Cell Press; 2020. pp. 737–741. https://doi.org/10.1016/j.immuni.2020.04.012 PMID: 32433946

11. Mahase E. Covid-19: Moderna vaccine is nearly 95% effective, trial involving high risk and elderly people shows. https://doi.org/10.1136/bmj.m4347 PMID: 33168562

12. Acuña-Zegarra MA, Díaz-Infante S, Baca-Carrasco D, Liceaga DO. COVID-19 optimal vaccination policies: a modeling study on efficacy, natural and vaccine-induced immunity responses. medRxiv. Cold Spring Harbor Laboratory Press; 2020; 2020.11.19.20235176. https://doi.org/10.1101/2020.11.19.20235176

13. Bartsch SM, O'Shea KJ, Ferguson MC, Bottazzi ME, Wedlock PT, Strych U, et al. Vaccine Efficacy Needed for a COVID-19 Coronavirus Vaccine to Prevent or Stop an Epidemic as the Sole Intervention. Am J Prev Med. Elsevier Inc.; 2020; 59: 493–503. https://doi.org/10.1016/j.amepre.2020.06.011 PMID: 32778354

14. Alvarez MM, González-González E, Trujillo-de Santiago G. Modeling COVID-19 epidemics in an Excel spreadsheet to enable first-hand accurate predictions of the pandemic evolution in urban areas. Sci Rep. Nature Research; 2021; 11: 4327. https://doi.org/10.1038/s41598-021-83697-w PMID: 33619337

15. Kermack W 0, Mckendrick AG. A contribution to the mathematical theory of epidemics. Proc R Soc London Ser A, Contain Pap a Math Phys Character. The Royal Society; 1927; 115: 700–721. https://doi.org/10.1098/rspa.1927.0118

16. Moein S, Nickaeen N, Roointan A, Borhani N, Heidary Z, Javanmard SH, et al. Inefficiency of SIR models in forecasting COVID-19 epidemic: a case study of Isfahan. Sci Rep. Nature Research; 2021; 11: 4725. https://doi.org/10.1038/s41598-021-84055-6 PMID: 33633275

17. Subramanian R, He Q, Pascual M. Quantifying asymptomatic infection and transmission of COVID-19 in New York City using observed cases, serology, and testing capacity. Proc Natl Acad Sci U S A. National Academy of Sciences; 2021; 118. https://doi.org/10.1073/pnas.2019716118 PMID: 33571106

18. Wölfel R, Corman VM, Guggemos W, Seilmaier M, Zange S, Müller MA, et al. Virological assessment of hospitalized patients with COVID-2019. Nature. Nature Research; 2020; 581: 465–469. https://doi.org/10.1038/s41586-020-2196-x PMID: 32235945

19. Singanayagam A, Patel M, Charlett A, Bernal JL, Saliba V, Ellis J, et al. Duration of infectiousness and correlation with RT-PCR cycle threshold values in cases of COVID-19, England, January to May 2020. Eurosurveillance. European Centre for Disease Prevention and Control (ECDC); 2020; 25: 2001483. https://doi.org/10.2807/1560-7917.ES.2020.25.32.2001483 PMID: 32794447

20. van Kampen JJA, van de Vijver DAMC, Fraaij PLA, Haagmans BL, Lamers MM, Okba N, et al. Duration and key determinants of infectious virus shedding in hospitalized patients with coronavirus disease-2019 (COVID-19). Nat Commun. Nature Research; 2021; 12: 1–6. https://doi.org/10.1038/s41467-020-20314-w PMID: 33397941

21. Quilty BJ, Clifford S, Hellewell J, Russell TW, Kucharski AJ, Flasche S, et al. Quarantine and testing strategies in contact tracing for SARS-CoV-2: a modelling study. Lancet Public Heal. Elsevier Ltd; 2021; 6: e175–e183. https://doi.org/10.1016/S2468-2667(20)30308-X PMID: 33484644

22. Zou L, Ruan F, Huang M, Liang L, Huang H, Hong Z, et al. SARS-CoV-2 Viral Load in Upper Respiratory Specimens of Infected Patients. N Engl J Med. Massachusetts Medical Society; 2020; 382: 1177–1179. https://doi.org/10.1056/NEJMc2001737 PMID: 32074444

23. Bai Y, Yao L, Wei T, Tian F, Jin D-Y, Chen L, et al. Presumed Asymptomatic Carrier Transmission of COVID-19. JAMA. 2020; https://doi.org/10.1001/jama.2020.2565 PMID: 32083643

24. MacIntyre CR. Global spread of COVID-19 and pandemic potential. Glob Biosecurity. University of New South Wales; 2020; 1. https://doi.org/10.31646/gbio.55

25. Home—Johns Hopkins Coronavirus Resource Center [Internet]. [cited 10 Sep 2020]. Available: https://coronavirus.jhu.edu/

26. Lewnard JA, Liu VX, Jackson ML, Schmidt MA, Jewell BL, Flores JP, et al. Incidence, clinical outcomes, and transmission dynamics of severe coronavirus disease 2019 in California and Washington: Prospective cohort study. BMJ. BMJ Publishing Group; 2020;369. https://doi.org/10.1136/bmj.m1923 PMID: 32444358

27. Guan W, Ni Z, Hu Y, Liang W, Ou C, He J, et al. Clinical Characteristics of Coronavirus Disease 2019 in China. N Engl J Med. Massachussetts Medical Society; 2020; 382: 1708–1720. https://doi.org/10.1056/NEJMoa2002032 PMID: 32109013

28. Pan L, Mu M, Yang P, Sun Y, Wang R, Yan J, et al. Clinical characteristics of COVID-19 patients with digestive symptoms in Hubei, China: A descriptive, cross-sectional, multicenter study. Am J Gastroenterol. Wolters Kluwer Health; 2020; 115: 766–773. https://doi.org/10.14309/ajg.0000000000000620 PMID: 32287140

29. Rosenbaum L. Facing Covid-19 in Italy—Ethics, Logistics, and Therapeutics on the Epidemic's Front Line. N Engl J Med. NLM (Medline); 2020; 382: 1873–1875. https://doi.org/10.1056/NEJMp2005492 PMID: 32187459

30. Bao L, Deng W, Gao H, Xiao C, Liu J, Xue J, et al. Reinfection could not occur in SARS-CoV-2 infected rhesus macaques. bioRxiv. Cold Spring Harbor Laboratory; 2020; 2020.03.13.990226. https://doi.org/10.1101/2020.03.13.990226

31. Prompetchara E, Ketloy C, Palaga T. Allergy and Immunology Immune responses in COVID-19 and potential vaccines: Lessons learned from SARS and MERS epidemic. https://doi.org/10.12932/AP-200220-0772 PMID: 32105090

32. Liu W, Fontanet A, Zhang P, Zhan L, Xin Z, Baril L, et al. Two-Year Prospective Study of the Humoral Immune Response of Patients with Severe Acute Respiratory Syndrome. J Infect Dis. Oxford University Press (OUP); 2006; 193: 792–795. https://doi.org/10.1086/500469 PMID: 16479513

33. Robinson E, Jones A, Lesser I, Daly M. International estimates of intended uptake and refusal of COVID-19 vaccines: A rapid systematic review and meta-analysis of large nationally representative samples. medRxiv. Cold Spring Harbor Laboratory Press; 2020; 2020.12.01.20241729. https://doi.org/10.1101/2020.12.01.20241729

34. Hasell Joe; Mathieu Edouard; Beltekian Diana; Macdonald Bobbie; Giattino Charlie; Ortiz-Ospina Esteban; et al. A cross-country database of COVID-19 testing. Sci data. 2020; 7: 1–7. Available: https://www.nature.com/articles/s41597-020-00688-8 https://doi.org/10.1038/s41597-019-0340-y PMID: 31896794